

# THE EFFECT OF SOLUTION HEAT TREATMENT ON AN ADVANCED NICKEL-BASE DISK ALLOY

J. Gayda, T. P. Gabb, and P. T. Kantzos

NASA Glenn Research Center  
Cleveland, Ohio 44135, USA

Keywords: Nickel-Base Superalloy, Disk, Heat Treatment

## Abstract

Five heat treat options for an advanced nickel-base disk alloy, LSHR, have been investigated. These included two conventional solution heat treat cycles, subsolvus/oil quench and supersolvus/fan cool, which yield fine grain and coarse grain microstructure disks respectively, as well as three advanced dual microstructure heat treat (DMHT) options. The DMHT options produce disks with a fine grain bore and a coarse grain rim. Based on an overall evaluation of the mechanical property data, it was evident that the three DMHT options achieved a desirable balance of properties in comparison to the conventional solution heat treatments for the LSHR alloy. However, one of the DMHT option, SUB/DMHT, produced the best set of properties, largely based on dwell crack growth data. Further evaluation of the SUB/DMHT option in spin pit experiments on a generic disk shape demonstrated the advantages and reliability of a dual grain structure at the component level.

## Introduction

Nickel-base superalloys intended for advanced disk applications require high creep resistance and dwell crack growth resistance in the rim region to withstand temperatures exceeding 650°C. However, they also require high strength and fatigue resistance in the bore and web regions which operate at temperatures of 500°C or less. In powder metallurgy disk superalloys having uniform grain microstructures, the former time-dependent properties at high temperature can be maximized with coarse grain microstructures produced by solution heat treatments above the  $\gamma'$  solvus temperature. The latter strength-dependent properties at intermediate temperatures can be maximized with fine grain microstructures produced by solution heat treatments below the  $\gamma'$  solvus. However, it follows that a disk having a uniform coarse grain microstructure will have compromised strength-dependent properties at intermediate temperatures in the bore and web. Conversely, a disk having a uniform fine grain microstructure will have compromised creep resistance and dwell crack growth resistance in the rim region. Therefore, an optimal disk would have a dual microstructure, consisting of fine grains in the bore and web with coarse grains in the rim.

Several approaches have been employed in order to solution heat treat disks to produce this type of dual microstructure. One approach (Ref. 1) uses induction heating to preferentially heat the rim of a single disk to above the  $\gamma'$  solvus temperature, while pressurized gas is run through the bore to keep the bore and web temperatures below the  $\gamma'$  solvus temperature. Another approach (Ref. 2) uses top and bottom pressurized caps over the bore of a single disk placed in a furnace at supersolvus temperature. The caps are used to blow pressurized cooling air through the center of the bore maintaining the bore and web below the  $\gamma'$  solvus temperature, while the rim heats to a supersolvus temperature. A new, lower cost approach developed at NASA (Ref. 3) uses carefully designed thermal blocks attached to the bore and web of a disk. The thermal blocks enhance the transient thermal gradient between the rim and bore allowing the rim to attain supersolvus solution temperature for sufficient time, while restricting the heat up of the bore and web to subsolvus temperatures. This dual microstructure heat treat approach allows improved disk performance with a small increase in disk cost compared to disks with a uniform microstructure.

Advanced powder metallurgy nickel-base disk alloys such as ME3 and Alloy 10 have been developed recently which also have the potential to improve performance of future gas turbine engines by allowing higher compressor discharge temperatures compared with today's gas turbine engines. Both of these alloys are produced using powder metallurgy and contain a high volume fraction of the  $\gamma'$  precipitate. ME3 was developed by GEAE, P&W, and NASA to have extended durability at 650°C in large engines with a low solvus temperature for enhanced processability (Ref. 4). Alloy 10 was developed by Honeywell Engines & Systems to produce superior tensile and creep capability in small engines at temperatures above 650°C (Ref. 5). This was achieved by using a high refractory element content, most notably tungsten. However, Alloy 10 also has a very high solvus temperature which makes supersolvus and dual microstructure heat treating challenging. Based on these alloys, NASA has developed a hybrid disk alloy, LSHR, which combines the low solvus of ME3 with the higher refractory element content of Alloy 10. This alloy has been shown to have a low solvus temperature, 1160°C, and tensile and creep properties which are superior to ME3 and comparable to Alloy 10 (Ref. 6).

The primary objective of this paper is to apply the advanced dual microstructure heat treatment process to an advanced disk alloy designed for such processing. The mechanical properties of the LSHR alloy given conventional solution heat treatments and advanced dual microstructure solution heat treatments will first be compared. The two conventional solution heat treatments, subsolvus/oil quench and supersolvus/fan cool, were designed to provide a fine grain high strength disk and a coarse grain creep resistant disk respectively. The advanced dual structure solution heat treatments were designed to produce a disk with a fine grain-high strength bore and coarse grain-creep resistant rim. The disks with a dual grain structure were produced using NASA's Dual Microstructure Heat Treatment (DMHT) technology (Ref. 3). High temperature spin testing on disks with selected solution heat treatments were then run to verify the performance advantage of DMHT technology on a component level.

### Materials and Procedures

Superalloy disks used in this study were produced from LSHR powder of the composition shown in Table 1. The

Table 1. Composition of LSHR in W/O.

Co	Cr	Al	Ti	W	Mo	Ta	Nb	C	B	Zr
21	13	3.5	3.5	4.3	2.7	1.6	1.5	.03	.03	.05

powder was produced by argon atomization and then screened, canned, compacted, and extruded to 15 cm diameter billet using a 6 to 1 reduction ratio. The billet was subsequently cut to mults and isothermally forged to a cylindrical shape 30cm in diameter and 5cm thick. As previously stated, the forgings were given a variety of solution heat treatments. For the conventional solution heat treatments, subsolvus and supersolvus, the following processing cycles were employed. An 1135°C/3hr/oil quench heat treatment was employed to produce a fine grain microstructure, ASTM 11, while an 1170°C/3hr/fan cooled heat treatment was employed to produce a coarse grain microstructure, ASTM 7. To develop a dual grain structure in a forging, the NASA DMHT technology was employed. The basic concept behind the DMHT technology utilizes the natural thermal gradients between the interior and exterior of a forging during the initial phase of a conventional heat treatment. By enhancing these thermal gradients with heat sinks, as shown in Figure 1, it is possible to design a solu-

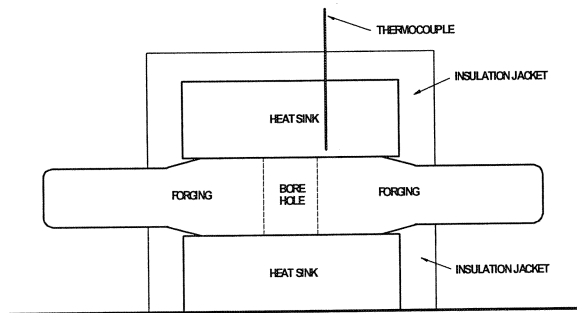


Figure 1. Schematic of DMHT assembly.

tion heat treatment which can produce a forging with the desired dual grain structure. The heat sinks consist of solid metal cylinders placed on the top and bottom faces of the forging. To enhance the effectiveness of the heat sinks an insulating jacket is employed to further slow the temperature rise of the central portion of the forging. To perform the heat treatment, the forging and heat sinks are placed in a furnace maintained at a temperature above the  $\gamma'$  solvus of LSHR and removed when the rim exceeds the solvus but before the bore reaches the solvus. After removal from the furnace the heat sinks are removed and the forging is cooled. The resulting dual grain structure of a typical forging is presented in Figure 2.

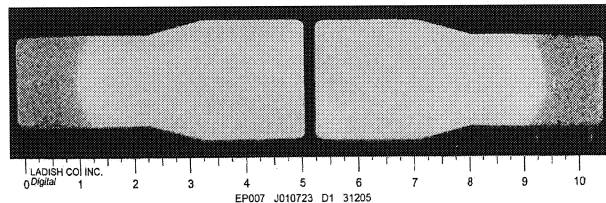


Figure 2. Typical macroetch of a DMHT forging.

Three DMHT options were studied. The first option employed a subsolvus solution heat treatment before the DMHT cycle. The second option employed a subsolvus solution heat treatment after the DMHT cycle. The third option consisted of a DMHT cycle without any subsolvus solution heat treatment. The heat treatment details of all forgings employed in this study are summarized in Table 2.

Table 2. Heat treatment of LSHR forgings.

FORGING ID	SOLUTION STEP 1	SOLUTION STEP 2	FINAL QUENCH
SUB/OIL	SUBSOLVUS	---	OIL
SUB/DMHT	SUBSOLVUS	DMHT	OIL
DMHT	DMHT	---	OIL
DMHT/SUB	DMHT	SUBSOLVUS	OIL
SUP/FAN	SUPERSOLVUS	---	FAN

Subsolvus solution heat treatments, in conjunction with the DMHT cycle, were employed to develop a bore grain size of ASTM 11. Without a subsolvus solution heat treatment, the bore grain size of the DMHT forging was found to be as fine as ASTM 13. Rim grain size of forgings with the dual grain structure, ASTM 6.5, were similar to the supersolvus forging, ASTM 7, with the exception of the SUB/DMHT forging. Its rim grain size was somewhat coarser at ASTM 5. All forgings were subsequently aged at 815°C for 8 hours to stabilize the  $\gamma'$  precipitate and carbide morphology.

Tensile, creep, fatigue, and crack growth specimens were machined from all forgings using identical cutup plans, for consistent specimen locations. Tensile, fatigue, and crack growth tests were run on bore specimens at 427°C, while creep and dwell crack growth tests were run on rim specimens at 704°C. Several forgings were also machined to the disk shape shown in Figure 3 to facilitate spin testing at elevated temperatures.

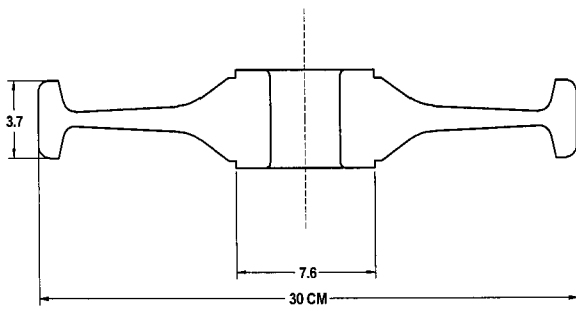


Figure 3. Disk shape employed for spin testing.

## Results & Discussion

Mechanical Properties. The temperatures selected for testing in this program, 427 and 704°C, are typical of bore and rim conditions intended in high pressure turbine disks for advanced gas turbine engines. The tensile data for the bore specimens are presented in Figure 4. As one might expect the

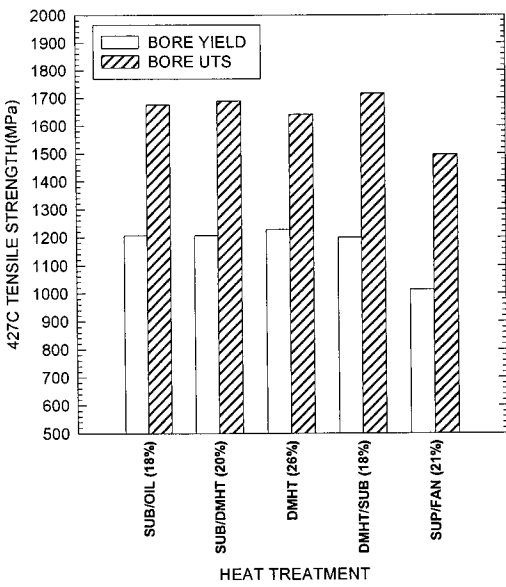


Figure 4. Tensile data for bore specimens. Elongation data in parenthesis.

the fine grain microstructures, subsolvus and the three DMHT options, show a significant strength advantage over the coarse grain, supersolvus microstructure. Further, the measured elongation values, for all heat treat options, were greater than 15% at 427°C.

Fatigue tests were run on bore specimens using a zero-tension, sinusoidal waveform with an applied strain range of 0.6%. This level is typical of the loading encountered at the bore of a high pressure turbine disk. The results of these tests are presented in Figure 5. As with tensile strength, the fine grain microstructures, subsolvus and the three DMHT options, exhibit markedly superior fatigue lives compared to

the coarse grain, supersolvus microstructure at this temperature. The shorter fatigue life of coarse grain,

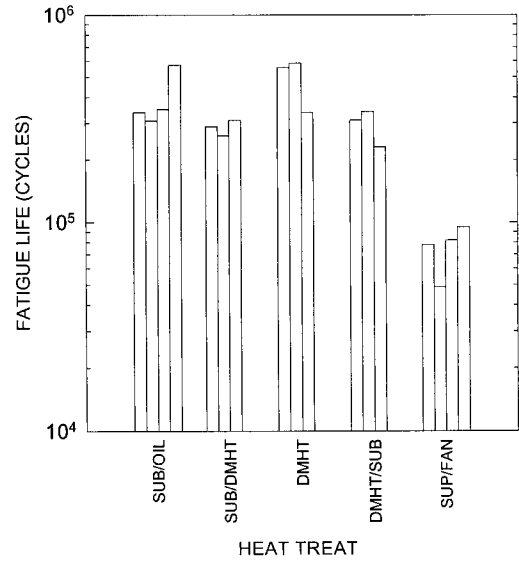


Figure 5. Bore fatigue data at 0.6% and 427°C.

supersolvus microstructures is often associated with accelerated crack initiation at facets associated with concentrated slip on octahedral planes of larger grains (Ref. 9).

Cyclic crack growth data, from  $K_b$  bar specimens, was generated using bore specimens obtained from each disk. Tests were run with an R-ratio of 0.05 after precracking at room temperature. As seen in Figure 6 there is little change

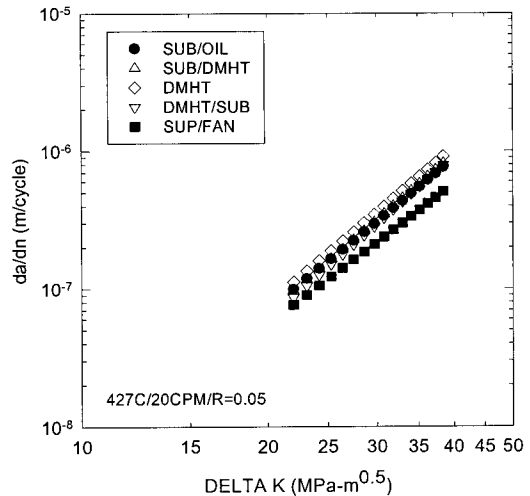


Figure 6. Cyclic crack growth rates of bore specimens at 427°C.

in the cyclic crack growth rate at 427°C, although the coarse grain, supersolvus microstructure does exhibit the slowest rate of crack growth.

Creep testing of rim specimens was performed at 704°C and 690MPa. The results of those tests are presented in Figure 7. As seen in that figure, the time to 0.2% creep was significantly longer for the coarse grain microstructures, supersolvus and the three DMHT options, than the fine grain, subsolvus microstructure. Additional creep testing, indicated that a coarse grain microstructure was superior at temperatures above 704°C, while a fine grain microstructure was superior at temperatures below 704°C.

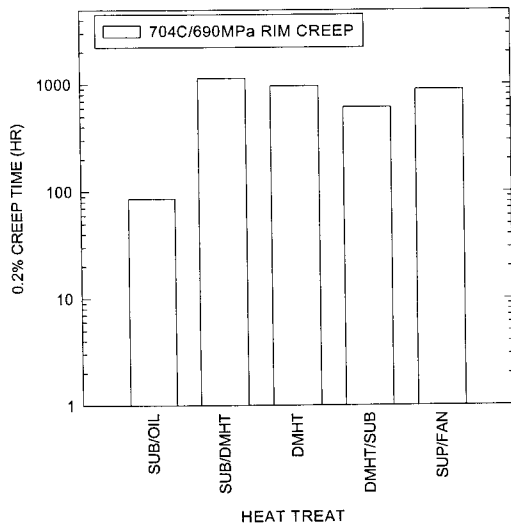


Figure 7. Creep data for rim specimens.

The final battery of tests run on the five heat treat options for LSHR was a dwell crack growth evaluation employing a 90 second dwell at peak load. Once again, a  $K_b$  bar specimen was employed to generate crack growth data. The results of these tests are summarized in Figure 8. Several interesting trends can be seen in this plot. First, the fine grain, subsolvus microstructure has the fastest crack growth rate. Second, there are significant differences among the coarse grain microstructures. The SUB/DMHT option has the slowest crack growth rate, while the DMHT/SUB option has the fastest crack growth rate among the coarse grain microstructures. Recall that the SUB/DMHT microstructure did exhibit the coarsest grain size, ASTM 5. Differences in grain size as well as cooling rates are thought to play a significant role in determining crack growth resistance (Ref. 10). The ranking of the present data appears to support the grain size hypothesis, however, the effect of cooling rate is somewhat perplexing as the fan cooled, supersolvus heat treatment did not yield the lowest crack growth rate. Clearly the DMHT options are complex, and require more work to understand the mechanisms governing the crack growth processes of these microstructures.

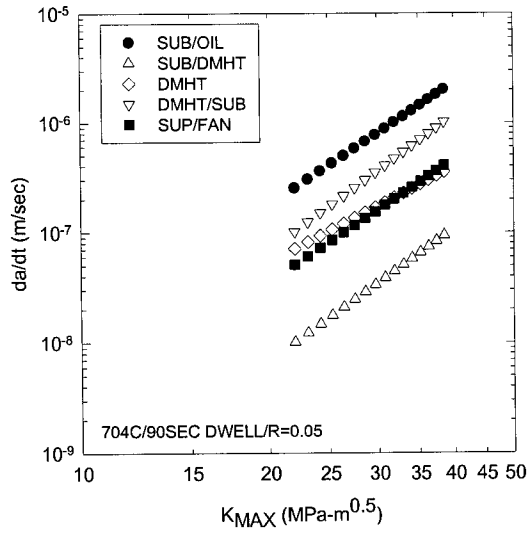


Figure 8. Dwell crack growth data for rim specimens.

Based on an overall evaluation of the mechanical property data, it is evident that the three DMHT options achieved a desirable balance of properties in comparison to the conventional solution heat treatments for the LSHR alloy. However, the SUB/DMHT option produced the best set of properties, largely based on the dwell crack growth data. For this reason, it was selected for further evaluation in spin pit experiments.

**Spin Testing.** Two spin pit experiments were performed on SUB/DMHT processed disks. In the first experiment, disk growth was measured after 12 hours at 815°C and 20000RPM. For comparative purposes a subsolvus disk was also run. In the second experiment, the 704°C burst strength of a SUB/DMHT processed disk was measured. In both experiments a generic disk shape, shown in Figure 3, was employed. This shape produces a uniform stress of maximum intensity in the web segment of the disk. The grain size transition zone was located in the web segment, approximately 5cm from the outer diameter of the disk.

The results of the high temperature disk growth experiments are presented in Figure 9. As seen in this plot, the experimentally measured growth (EXP) of the SUB/DMHT processed disk was significantly less than the subsolvus disk run under identical conditions. Further, the results of this experiment could be predicted using a 2-D, viscoelastic finite element analysis (FEA) using the following power law creep expressions for fine grain and coarse grain material, based on the creep specimen test data:

$$\Delta\epsilon/\Delta t = A\sigma^4$$

$$A_{FINE} = 1.8e^{-17} \text{ sec}^{-1} \text{ MPa}^{-4}$$

$$A_{COARSE} = 2.5e^{-19} \text{ sec}^{-1} \text{ MPa}^{-4}$$

The values for A in these analyses were obtained from creep data for the LSHR alloy at 815°C. A detailed explanation of

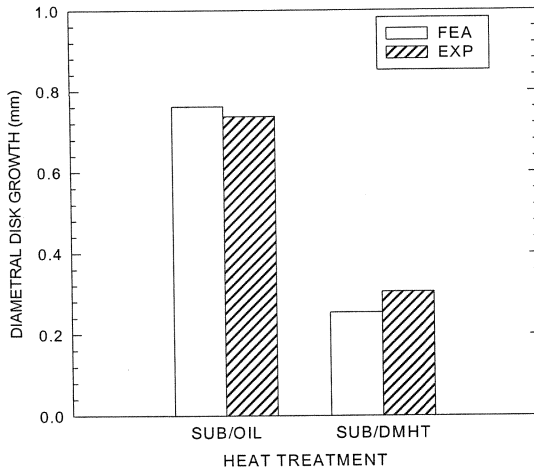


Figure 9. Disk growth after 12 hours at 815°C and 20000RPM. Web stress is approximately 350MPa.

the FEA model can be found in Reference 11. This experiment and analysis clearly demonstrates enhanced resistance to creep growth at high temperatures when the LSHR disk has a dual grain structure with a coarse grain rim.

High temperature burst testing of the SUB/DMHT processed disk was then performed. The test was run in an incremental manner so plastic growth of the disk could be measured and compared with finite element predictions. The disk was spun to speeds of 35000, 38000, and 40000RPM before running to failure. After each of the first three trials the disk was cooled and removed from the pit to measure plastic growth. To minimize creep deformation in each of these trials, the speed was increased at a rate of 5000RPM every minute. On the fourth spin trial, the disk burst at a speed of 42530RPM. As seen in Figure 10, the failure location was about 2.5cm from the outer periphery of the disk, placing it in the coarse grain region. Finite element analysis of the spin testing was performed using a 2-D axisymmetric model. Two material groups were employed in this analysis, representing the fine

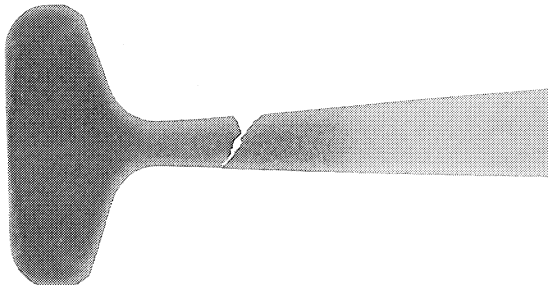


Figure 10. Etched cross section of burst disk showing failure location in coarse grain region.

grain and coarse grain microstructure. In both cases a bilinear, elastic-plastic material response was assumed. The values for yield stress, used in the analysis, were obtained from tensile data for the LSHR alloy at 704°C, 1170MPa for fine grain material and 1100MPa for coarse grain material. Analyses were run at 35000, 38000, 40000, and 42000RPM. As the stress state is multiaxial, the magnitude of the von Mises stress was examined. At 42000RPM the peak stress reached 1400MPa in the web, as shown in Figure 11.

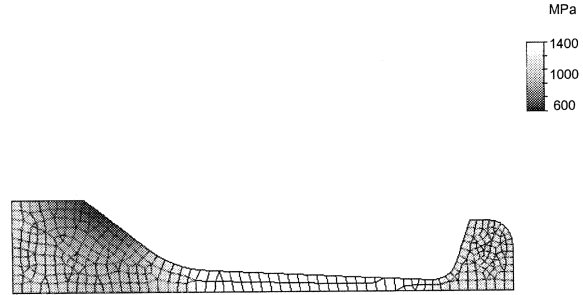


Figure 11. Predicted stress distribution in the disk at 42000RPM.

The disk would be expected to burst at this speed as the ultimate tensile strength of the alloy has been reached. To verify the accuracy of the stress distributions, the predicted growth of the disk is compared with experimentally measured growth of the disk in Figure 12. In general, the comparison is quite good thereby verifying the accuracy of the stress distribution in Figure 11.

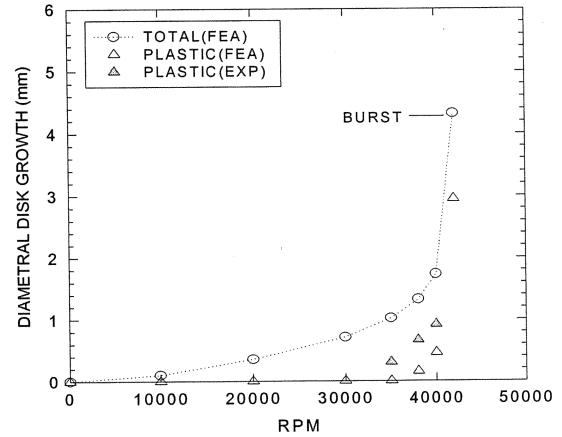


Figure 12. Growth of disk during burst testing.

From this test, one would conclude that the SUB/DMHT processed disk met or exceeded expectations for several reasons. First, the disk failed near the predicted speed. Second, significant growth of the disk occurred before failure. Lastly, the fracture appeared to be ductile in nature as seen in Figure 13.

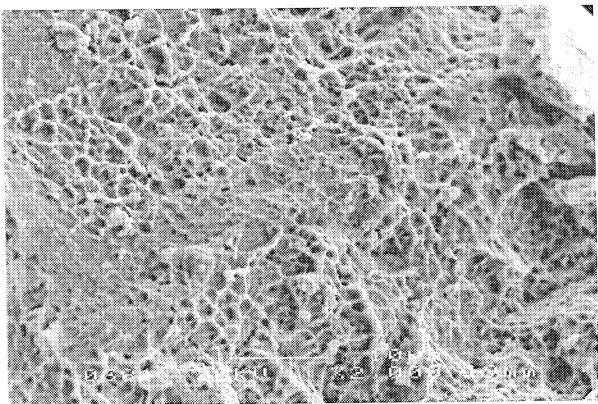


Figure 13. Fracture surface of burst disk.

### Summary & Conclusions

Five heat treat options for an advanced nickel-base disk alloy, LSHR, have been investigated. These included, two conventional solution heat treat cycles, subsolvus and supersolvus, which yielded uniform fine grain and coarse grain microstructure disks respectively, as well as three advanced dual microstructure heat treat (DMHT) options. The first option employed a subsolvus solution heat treatment before the DMHT cycle. The second option employed a subsolvus solution heat treatment after the DMHT cycle. The third option consisted of a DMHT cycle without any subsolvus solution heat treatment. Each DMHT option produced a disk with a fine grain bore and a coarse grain rim. Based on an overall evaluation of the mechanical property data, it was evident that the three DMHT options achieved a desirable balance of properties in comparison to the conventional solution heat treatments for the LSHR alloy. Each of the three DMHT options had high strength, fatigue resistant bores and creep resistant rims. However, the SUB/DMHT option produced the best set of properties, largely based on dwell crack growth data. Further evaluation of the SUB/DMHT option in spin pit experiments on a generic disk shape demonstrated the advantages and reliability of a dual grain structure at the component level. These spin pit experiments included an 815°C creep growth test as well as a 704°C burst test.

### References

1. G. Mathey, "Method of Making Superalloy Turbine Disks Having Graded Coarse and Fine Grains", U.S. Patent 5,312,497, May, 1994.
2. S. Ganesh and R. Tolbert, "Differentially Heat Treated Article and Apparatus and Process for the Manufacture Thereof ", U. S. Patent 5,527,020, June, 1996.
3. J. Gayda, T. P. Gabb, and P. T. Kantzos, "Heat Treatment Devices and Method of Operation Thereof to Produce Dual Microstructure Superalloy Disks ", U. S. Patent 6,660,110, December, 2003.
4. J. Gayda, T. P. Gabb, P. T. Kantzos, and D. U. Furrer, Heat Treatment Technology for Production of Dual Microstructure Superalloy Disks, NASA TM 2002-211558, April 2002.
5. J. Gayda, D. U. Furrer, "Dual Microstructure Heat Treatment", Advanced Materials & Processes, July, 2003.
6. T. P. Gabb, J. Telesman, P. T. Kantzos, and K. O'Connor, Characterization of the Temperature Capabilities of Advanced Disk Alloy ME3, NASA TM 2002-211796, August 2002.
7. H. Merrick, R. Benn, and P. Bhowal, U. S. Patent 6468368, Washington D.C., 2002.
8. T. P. Gabb, J. Gayda, J. Telesman, P. T. Kantzos, and W. Konkel, Realistic Subscale Evaluations of the Mechanical Properties of Advanced Disk Superalloys, NASA TM 2003-212086, January 2003.
9. T. P. Gabb, J. Gayda, and J. Sweeney, The Effect of Boron on the Low Cycle Fatigue Behavior of Disk Alloy KM4, NASA TM 2000-210458, September, 2000.
10. FCG reference.
11. J. Gayda and P. T. Kantzos, High Temperature Spin Testing of a Superalloy Disk with a Dual Grain Structure, NASA TM 2002-211684, June 2002.